

## Test of the Independence Postulate in the Bohr Theory of Compound-Nucleus Decay: $^{50}\text{Cr}^*$ System<sup>†</sup>

Man King Go<sup>‡</sup> and Samuel S. Markowitz

*Department of Chemistry and Lawrence Berkeley Laboratory, University of California, Berkeley, California 94720*

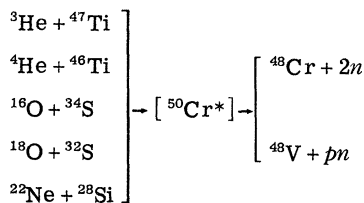
(Received 13 September 1972)

Excitation functions for the production of  $^{48}\text{V}$  and  $^{48}\text{Cr}$  from incident ions  $^3\text{He}$ ,  $\alpha$ ,  $^{16}\text{O}$ ,  $^{18}\text{O}$ , and  $^{22}\text{Ne}$  involving the compound system  $^{50}\text{Cr}^*$  have been measured. Test of the independence postulate was performed in a Ghoshal type of experiment. Effects of the nuclear Coulomb barrier and high reaction  $Q$  value upon the two-nucleon evaporation excitation functions were noted. For all the reaction pairs, the  $^{48}\text{V}$  production is more than a factor of 10 bigger than the corresponding  $^{48}\text{Cr}$  cross section. This phenomenon can be explained by the effect of odd-even nucleon number of the product nucleus. Simple calculations of the angular momentum and rotational energy of the compound nucleus were performed. The energy shift of the excitation function can be explained by the effect of angular momentum. The reactions involved were found to be generally consistent with the compound-nucleus model.

### I. INTRODUCTION

One of the important theories concerning nuclear reactions in the intermediate energy region (<10 MeV per incident nucleon) is the compound-nucleus model.<sup>1</sup> In this model, the decay of the compound nucleus is independent of its mode of formation. Since the work by Ghoshal<sup>2</sup> in which the decay of the  $^{64}\text{Zn}^*$  compound nucleus formed with protons was compared with that formed with  $\alpha$  particles, many investigations<sup>3-7</sup> have been performed along the same line. In most cases, the independence postulate is upheld roughly. More recently, when comparing the reaction excitation functions, care has been taken to match not only the excitation energy of the compound nucleus, but also its angular momentum.<sup>8,9</sup> However, very few investigations have compared heavy-ion-induced reactions with those induced by light projectiles (such as  $p, n, ^3\text{He}, \alpha$ ). It is felt that the independence postulate can be subjected to a more severe test when comparing reactions involving vastly different reactants.

In this work, the compound nucleus  $^{50}\text{Cr}^*$  is formed by different entrance channels and the decay of this compound nucleus is observed through products from  $pn$  and  $2n$  emissions. The reactions are given below:



In all the reactions studied, the excitation energy of the compound nucleus is less than 60 MeV.

### II. EXPERIMENTAL PROCEDURES

A stacked-foil method was used. Target foils and aluminum degrader foils were interspaced in a target holder and bombarded with appropriate ion beams from particle accelerators. For  $^3\text{He}$  and  $\alpha$  bombardments, the Berkeley 88-in. cyclotron was used, whereas the Berkeley heavy ion linear accelerator was used for the source of heavy ions. The beam intensity was measured to within  $\pm 1\%$  with a Faraday cup connected to an integrating electrometer. The  $^3\text{He}$  or  $^4\text{He}$  beam was magnetically analyzed, so that the incident energy is known accurately. For the heavy ion beams, the full energy ( $10.4 \pm 0.2$  MeV/nucleon) was used. The energy at various positions in the stack was determined with conventional range-energy curves. For  $^3\text{He}$  and  $^4\text{He}$ , the tables of Williamson, Boujot, and Picard<sup>10</sup> were used; while for the heavy ions, the range-energy curves were calculated with a computer code by Steward.<sup>11</sup>

The targets used were prepared by vacuum evaporation of natural materials or enriched isotopes obtained from Oak Ridge National Laboratory. The backing and recoil catcher for the targets is thin Al foil ( $1.6 \text{ mg/cm}^2$ ). Mass analysis and chemical impurity of the target materials are presented in Table I. To prevent sublimation or loss of sulfur material during bombardment, a thin ( $\sim 100\text{-}\mu\text{g/cm}^2$ ) aluminum layer was evaporated on top of the sulfur deposit to serve as a protective shield and heat conductor.

$\gamma$  spectroscopy was used to identify and measure the radioactivity produced. Two Ge(Li) semiconductor  $\gamma$ -ray detectors were employed. The active volumes are 7 and 14  $\text{cm}^3$  with resolutions, respectively, of 2.5 and 1.4 keV (full width at half

maximum) for the 122 keV  $^{57}\text{Co}$   $\gamma$  ray. The  $\gamma$ -ray spectra from the 1024-channel analyzer were recorded in 7-in.-reel magnetic tapes.  $\gamma$ -spectra photopeak analyses were handled by the CDC-6600 computer with the code SAMPO.<sup>12</sup> Energy and efficiency calibration of the  $\gamma$ -ray detection systems were facilitated with a set of eight absolute  $\gamma$ -ray standards.<sup>13</sup>

The radioactivities of  $^{48}\text{Cr}$  and  $^{48}\text{V}$  were determined with the 116-keV (98%) and the 938-keV (100%)  $\gamma$  rays, respectively. Graphical analysis of the decay curves is adequate to obtain the decay rates at the end of bombardment. The decay rates were converted to absolute cross sections by making appropriate corrections for beam intensities, saturation effects during bombardment, and detector efficiencies.

### III. EXPERIMENTAL RESULTS

Excitation functions for the various reactions are given in Fig. 1. The contributions to the cross sections from other isotopes in the target are very small by isotopic-abundance arguments and experiments involving targets enriched in the suspected isotopes. Contribution of the  $^{48}\text{V}$  activity from the decay of the  $^{48}\text{Cr}$  has been subtracted.

In all the five cases, the cross sections ( $x, pn$ ) are about 13 times that of ( $x, 2n$ ), here  $x$  stands

for any of the five projectiles. The same enhancement of proton-emission cross section has been observed by several authors.<sup>2, 14, 15</sup> The greater emission probability can be explained by the difference in the level density of the product nuclei. The nucleus  $^{48}\text{V}$  is odd-odd, and is expected<sup>16</sup> to have many more levels available, at equal excitation energies, than the  $^{48}\text{Cr}$ , an even-even nucleus. Since there are more channels available for the compound nucleus to decay to  $^{48}\text{V}$ , enhancement of proton evaporation results.

The excitation functions for the  $^4\text{He}$  reactions agree reasonably with those obtained by Raleigh.<sup>17</sup>

## IV. CALCULATIONS AND DISCUSSION

### A. Comparison of Excitation Functions

In the classical test of the independence postulate, the excitation functions from different reactions involving the same compound nucleus forming the same product are compared in a plot where the excitation energy is one of the axes.

Before performing such a comparison, we wish to point out that some nuclear reactions are strongly suppressed by the Coulomb barrier and should not be compared with others not so suppressed. The excitation energy of the  $^{50}\text{Cr}^*$  compound nucleus from the  $^{18}\text{O} + ^{32}\text{S}$  reaction near the Coulomb barrier is about 45 MeV. The excitation function

TABLE I. Mass analysis and chemical composition of target material.

Target	Mass analysis		Chemical impurities	
	Mass number	(%)	(maximum)	(%)
Titanium-46 ( $\text{TiO}_2$ )	46	81.2	Ca	<0.01
	47	2.1	Fe	<0.05
	48	14.5	Si	<0.07
	49	1.1	W	<0.05
	50	1.1	Others negligible	
Titanium-47 ( $\text{TiO}_2$ )	46	1.9	Fe	<0.02
	47	79.5	Si	<0.03
	48	16.5	Others negligible	
	49	1.1		
	50	1.0		
Sulfur-34	32	65.9	Zn	<0.02
	33	0.57	Al, Cd, Cr, Cs, Ge, Ni,	
	34	33.5	Pt, W, Zr, each	<0.05
	36	0.05		
Sulfur (natural)	32	95.0		
	33	0.76		
	34	33.5	Negligible	
	36	<0.014		
Silicon (natural)	28	92.2		
	29	4.7	Negligible	
	30	3.1		

for two-nucleon evaporation is expected to have peaked and become small. The shape of the excitation function observed is probably due to the increasing penetration of the Coulomb barrier and the decreasing probability for two-nucleon evaporation as excitation energy is increased. Figure 2 shows a comparison of the excitation functions for  $2n$  and  $pn$  evaporation from  $^{16}\text{O} + ^{34}\text{S}$  and  $^{18}\text{O} + ^{32}\text{S}$  reactions.

The corresponding cross section for the  $^{18}\text{O}$ -induced reactions is a factor of 10 less than the  $^{16}\text{O}$ -induced reaction; and the peaks of the  $^{18}\text{O}$  excitation functions are displaced about 9 MeV toward higher excitation energies. The discrepancy should not be taken as evidence against the independence postulate, because this effect is mainly due to the Coulomb barrier.

Because the  $^{22}\text{Ne}$  excitation functions studied are

also strongly suppressed by the Coulomb barrier, we wish to compare the cross sections of the other three reacting pairs. Figure 3 shows the comparison of the  $^3\text{He}$ ,  $\alpha$ , and  $^{16}\text{O}$ -induced two-nucleon-emission excitation functions.

In the classical test of the independence postulate, the comparison must be made after the cross sections have been normalized with respect to the total reaction cross sections. However, the  $^3\text{He}$  and  $^{16}\text{O}$  excitation functions are near the Coulomb barrier, and the calculation of total reaction cross section in this region by the optical model<sup>18</sup> is very sensitive to the parameters used. Furthermore, as of now, there are no experimentally determined optical parameters available for the reaction studied. The following procedure is used to facilitate the comparison. The magnitude of the cross sections for the ( $^3\text{He}, pn$ ) and ( $^{16}\text{O}, pn$ ) reactions were

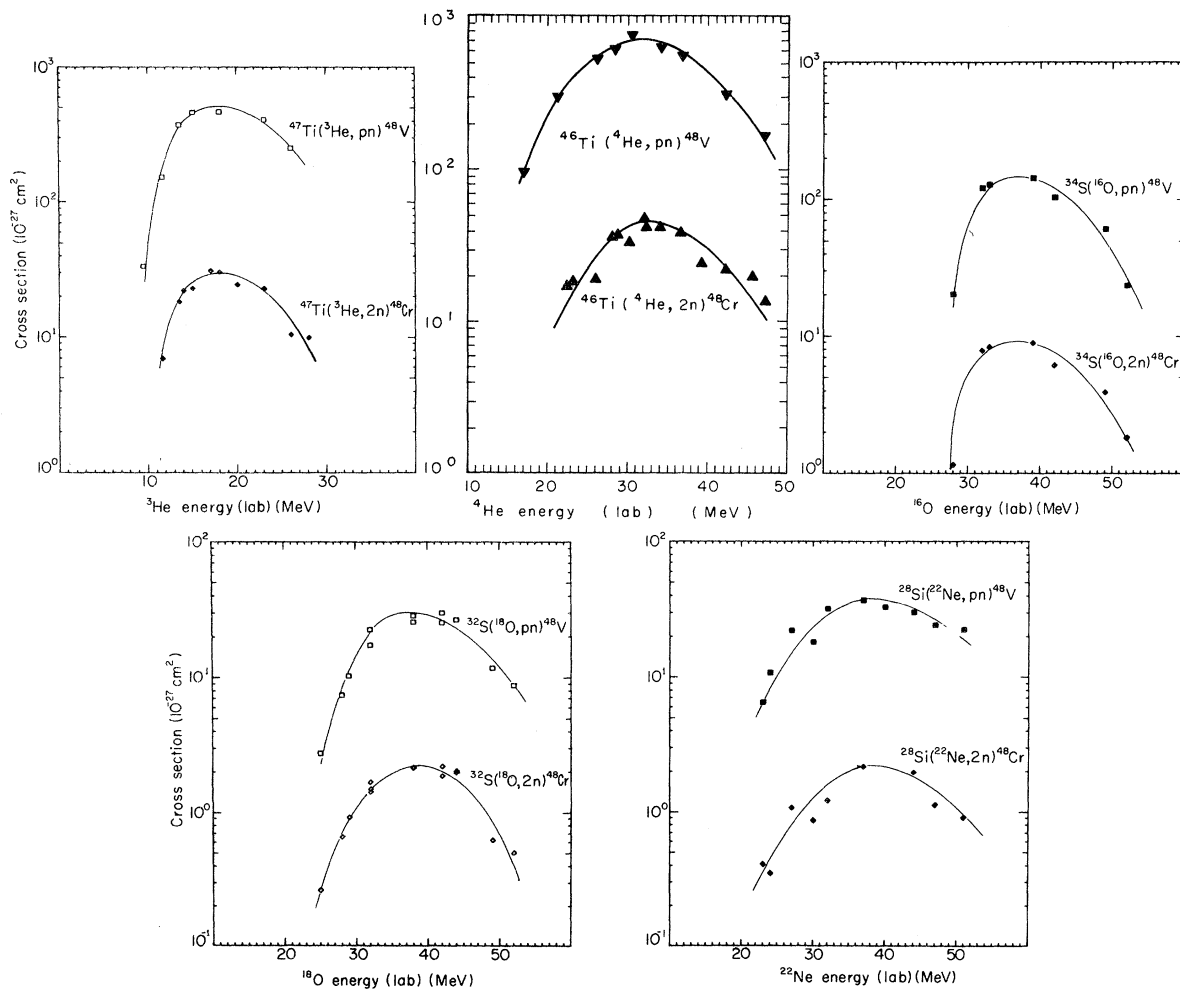


FIG. 1. Experimental excitation functions for the production of  $^{48}\text{V}$  and  $^{48}\text{Cr}$  from various charged particles involving the compound nucleus  $^{50}\text{Cr}^*$ . The solid lines are drawn only to aid the eyes and have no theoretical significance.

arbitrarily increased so that they are about equal to the  $(\alpha, pn)$  excitation function at the peak position. The  $({}^3\text{He}, 2n)$  and  $({}^{16}\text{O}, 2n)$  cross sections were also increased the same percentage as the respective  $pn$  excitation functions. The result is shown in Fig. 4.

It is interesting to compare the excitation functions from  ${}^{22}\text{Ne}$  and  ${}^{18}\text{O}$  reactions. All these cross sections are severely suppressed by the Coulomb barrier, and presumably arise from the evaporation of high-energy neutrons and protons. Figure 5 shows such a comparison.

The  $({}^{18}\text{O}, 2n)$  and  $({}^{18}\text{O}, pn)$  excitation functions have the same shape and the same magnitude as the corresponding excitation functions from  ${}^{22}\text{Ne} + {}^{28}\text{Si}$ . However, the  ${}^{18}\text{O}$  cross sections are shifted about 5.5 MeV toward higher excitation energy. This shift in energy can be explained by angular momentum effects.

#### B. Effects of Angular Momentum

The effects of angular momentum upon the de-excitation of the compound nucleus have attracted increasing attention.<sup>19-24</sup> Generally, the evaporation of particles will release from the compound nucleus a large amount of excitation energy but small amount of angular momentum, because of the large binding energy and relatively small kinetic energy of the emitted particle. However, for any given angular momentum, there is an en-

ergy limit<sup>25</sup> below which no available level exists. If the decay of the compound nucleus with large initial angular momentum is only by particle emission, the compound nucleus will reach a situation where it will have relatively low excitation energy and high angular momentum. This compound nucleus then will possess enough excitation energy to emit another particle, but there is no available level with the necessarily high angular momentum in the residual nucleus, and thus the emission of that particle is prohibited. In this case, deexcitation must proceed via  $\gamma$ -ray emission. This de-excitation by  $\gamma$  rays essentially removes some of the available excitation energy; thus the excitation function will be shifted toward higher excitation energies.

An alternative view is developed by Ericson and Strutinski.<sup>26</sup> In this treatment the rotational energy of the compound nucleus is considered to be unavailable for deexcitation by particle emission, and the true internal excitation energy  $E^\dagger$  is given by

$$E^\dagger = E^* - E_r, \quad (1)$$

where  $E^*$  and  $E_r$  are the excitation energy and rotational energy, respectively.

Attempts will be made to estimate the rotational energy of the compound nucleus and compare it to the experimentally observed energy shift of the excitation functions. The rotational energy of the

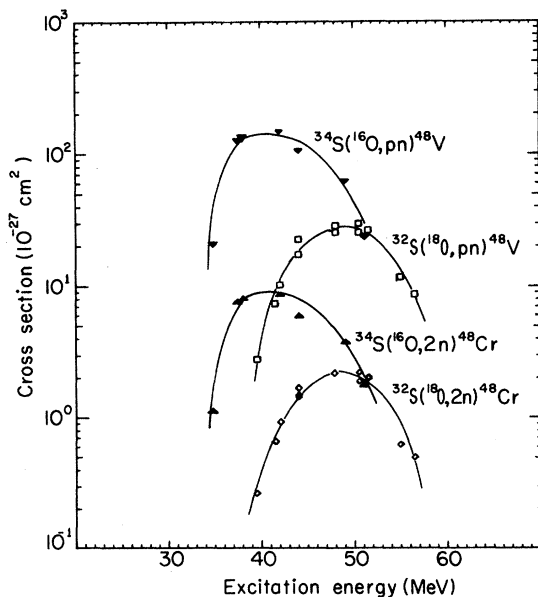


FIG. 2. Comparison of the excitation functions from  ${}^{18}\text{O}$ - and  ${}^{16}\text{O}$ -induced reactions. The difference in magnitude of these cross sections can be attributed to Coulomb-barrier effects.

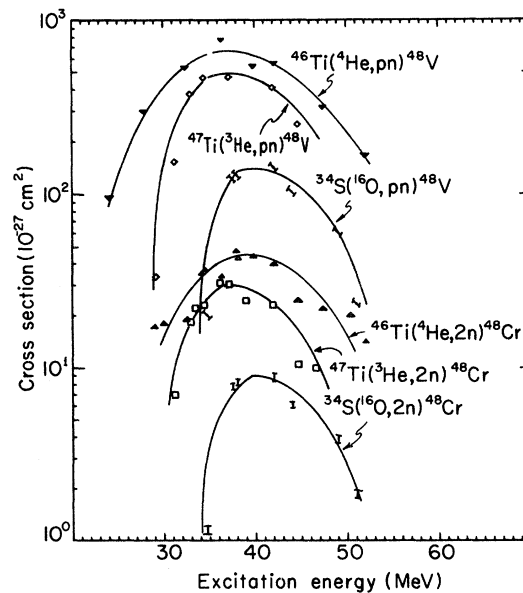


FIG. 3. Three-way comparison of the  $2n$  and  $pn$  evaporation excitation functions from  ${}^3\text{He} + {}^{47}\text{Ti}$ ,  ${}^4\text{He} + {}^{46}\text{Ti}$ , and  ${}^{16}\text{O} + {}^{34}\text{S}$  reactions.

compound nucleus is<sup>22</sup>

$$E_r = \frac{\hbar^2}{2\mathcal{I}} \langle J(J+1) \rangle, \quad (2)$$

where  $\mathcal{I}$  is the moment of inertia of the compound nucleus,  $J$  is the spin of the compound nucleus, and  $\hbar$  is Planck's constant/ $2\pi$ . The moment of inertia of the compound nucleus is usually approximated by its high excitation limit, the moment of inertia of the rigid sphere.<sup>26</sup>

In order to calculate the average angular momentum quantum number  $\langle J(J+1) \rangle$ , the distribution of angular momentum for the compound nucleus as a function of energy is needed.

The cross section for the formation of a compound nucleus with angular momentum  $J_C$  at bombarding  $E$  is<sup>27</sup>

$$\sigma(J_C, E) = \pi\lambda \sum_{s=|I-s|}^{I+s} \sum_{l=|J_C-s|}^{J_C+s} \frac{2J_C+1}{(2s+1)(2l+1)} T_l(E), \quad (3)$$

where  $\lambda$  is the deBroglie wavelength of the incident particle,  $I$  is the spin of the target nucleus,  $s$  is the spin of the projectile, and  $T_l(E)$  is the transmission coefficient of the projectile with orbital angular momentum  $l$  and energy  $E$ .

There is a maximum angular momentum  $J_C(\max)$  for the compound nucleus at an energy,  $J_C(\max) = l_{\max} + s + I$ , where  $l_{\max}$  is chosen so that  $T_{l_{\max}} > 10^{-6}$ .

The probability  $P_{J_C}$  for the formation of a com-

pound nucleus with spin  $J_C$  is simply

$$P_{J_C} = \frac{\sigma(J_C, E)}{\sum_{J_C=0}^{\infty} \sigma(J_C, E)}. \quad (4)$$

From  $P_{J_C}$  the average angular momentum quantum number can be calculated. Hafner, Huizenga, and Vandenbosch<sup>28</sup> have written a computer code ISOMER to calculate the average angular momentum of the compound nucleus. The ISOMER program requires as its input the spin of the target and projectile, the deBroglie wavelength of the incident particle, and the transmission coefficients for the projectile of different  $l$  at  $E$ .

The transmission coefficients can be approximated by a method given by Thomas.<sup>29</sup> The interaction between the target and projectile can be approximated by a diffuse potential

$$V(r, l) = \frac{Z_1 Z_2 e^2}{r} + \frac{\hbar^2}{2\mu r^2} l(l+1) - 67 \exp\left[\frac{r - 1.17(A_1^{1/3} + A_2^{1/3})}{-0.574}\right], \quad (5)$$

where  $Z$  and  $A$  refer to charge and mass, the subscripts 1 and 2 refer to projectile and target, respectively. This potential is further approximated by a parabola with matching position, height, and curvature at its maximum. The transmission co-

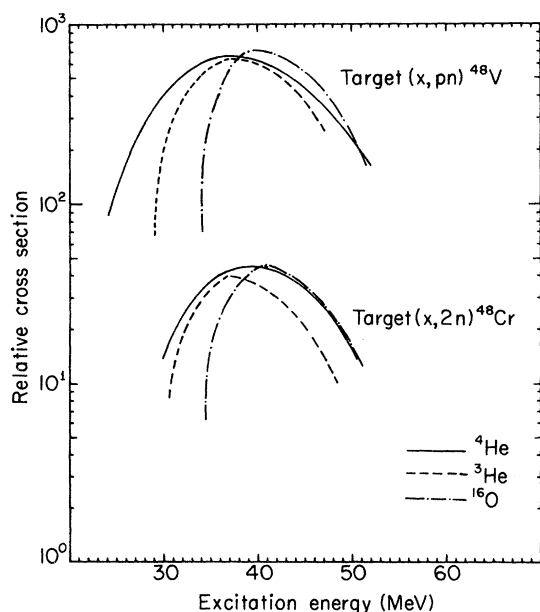


FIG. 4. Three-way comparison of the  $2n$  and  $pn$  evaporation excitation functions after arbitrarily shifting the magnitude of the  $^{16}\text{O}$  and  $^3\text{He}$  cross sections (see text).

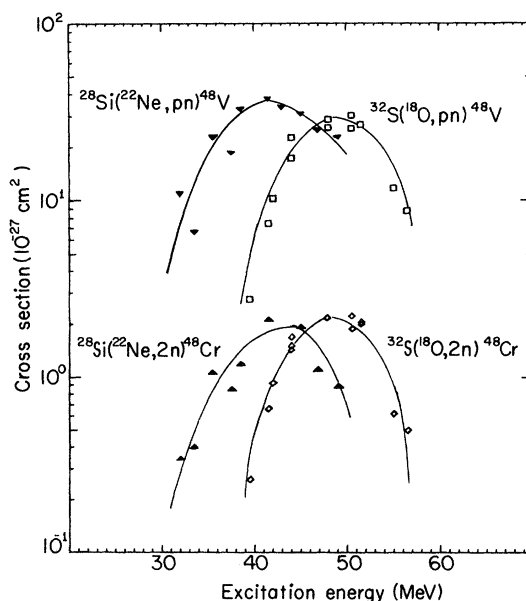


FIG. 5. Comparison of the  $2n$  and  $pn$  emission excitation functions from the  $^{18}\text{O} + ^{32}\text{S}$  and  $^{22}\text{Ne} + ^{28}\text{Si}$  reactions. All these cross sections are suppressed severely by the Coulomb barrier.

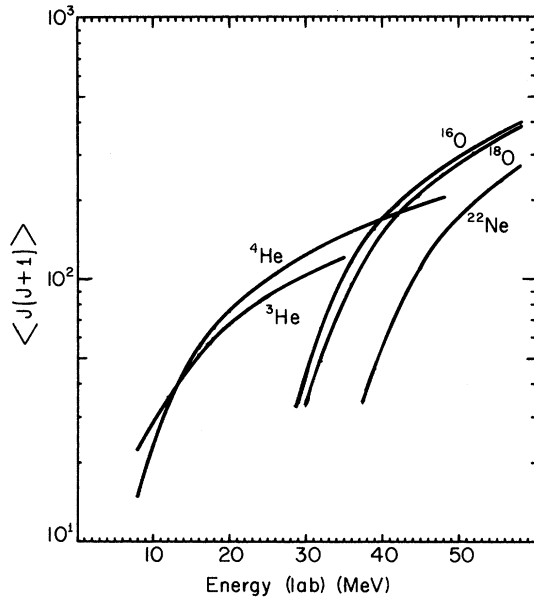


FIG. 6. Calculated average angular momentum quantum number for the  $^{50}\text{Cr}^*$  compound nucleus as a function of bombarding energy for various reactant pairs.

efficients for the parabola are given by Hill and Wheeler.<sup>30</sup>

The calculated angular momentum for the various reactant pairs is presented in Fig. 6. With Eq. (2) and Fig. 6, the rotational energy of the compound nucleus can be calculated. At the peak position of the  $(\alpha, pn)$  and  $(\alpha, 2n)$  excitation functions, the bombarding energy is about 31 MeV. The  $\langle J(J+1) \rangle$  value is 130 and the rotational energy is 6.4 MeV. For the  $(^{16}\text{O}, 2n)$  and  $(^{16}\text{O}, pn)$  excitation functions, the rotational energy at the peak is 7.4 MeV. The expected energy shift between the  $^{16}\text{O}$ - and  $\alpha$ -induced reactions will therefore be 1 MeV. The observed shift is about 2 MeV. This discrepancy may be caused by the Coulomb barrier acting on the low-energy edge of the  $^{16}\text{O}$  excitation functions.

For the  $^{22}\text{Ne}$ -induced reactions, the rotational energy at the peak of the two-nucleon-evaporation excitation functions is about 2.0 MeV, and the  $^{18}\text{O}$ -induced reactions  $E_r$  is 5.9 MeV. The expected displacement is about 3.9 MeV. The observed shift is 5.5 MeV.

Although the calculated energy shifts do not agree perfectly with the observed ones, these approximate calculations do allow qualitative understanding of the effect of angular momentum upon the deexcitation of the compound nucleus. Better agreement can be achieved if the moment of inertia of the rotating compound nucleus is taken to be  $^7 k \mathcal{I}_r$ , where  $k$  is a parameter, and  $\mathcal{I}_r$  is the moment of

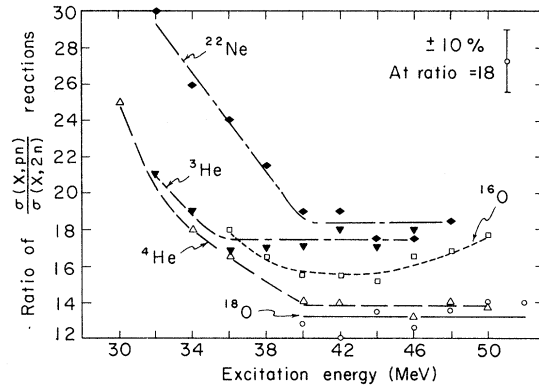


FIG. 7. Ratio of  $\sigma(x, pn)$  to  $\sigma(x, 2n)$  reaction from  $^{50}\text{Cr}^*$ . The lines are to guide the eye. A 10% error bar is shown.

inertia of a rigid sphere. For more accurate and realistic calculations, the treatment involves the detailed calculation of the  $\gamma$ -ray deexcitation and spin distribution<sup>31</sup> of the decaying compound nucleus.

For the compound nucleus reaction  $a+A \rightarrow C^* \rightarrow b+B$ , according to the independence postulate, the cross section can be formulated as

$$\sigma(a, b) = \sigma_c(a)P(C, b), \quad (6)$$

where  $\sigma_c(a)$  is the cross section for the formation of the compound nucleus  $C^*$  from the entrance channel  $a+A$ ;  $P(C, b)$  is the probability that the compound nucleus decays through the exit channel  $b+B$ .  $P(C, b)$  depends only on the exit channel and the compound nucleus.

Furthermore, for reactions involving different exit channels, we have

$$\frac{\sigma(a, b)}{\sigma(a, d)} = \frac{\sigma_c(a)P(C, b)}{\sigma_c(a)P(C, d)} = \frac{P(C, b)}{P(C, d)}, \quad (7)$$

where  $\sigma(a, d)$  designates the reaction cross section for the reaction  $a+A \rightarrow C^* \rightarrow d+D$ . Because  $P(C, b)$  and  $P(C, d)$  do not depend on the entrance channel, the ratio of cross sections from different entrance channels should be equal,<sup>32</sup> or,

$$\frac{\sigma(a, b)}{\sigma(a', b)} = \frac{P(C, b)}{P(C, d)} = \frac{\sigma(a', b)}{\sigma(a', d)}, \quad (8)$$

where  $\sigma(a', b)$  is the cross section for the reaction  $a'+A' \rightarrow C^* \rightarrow b+B$ ; similarly for  $\sigma(a', d)$ .

Figure 7 shows the ratios of  $pn$  cross sections to the  $2n$  cross sections for all the reactant pairs studied. Although the ratios lie mainly between 12 and 18, it is obvious that Eq. (8) is not strictly upheld. For a more quantitative comparison, effects of isospin,<sup>33</sup> Coulomb barrier, and  $\gamma$ -ray competition<sup>34</sup> on the decay of the compound nucleus must be taken into account.

†Work performed under the auspices of the U. S. Atomic Energy Commission.

‡Submitted in partial fulfillment of the Ph.D. requirements at the Department of Chemistry, University of California, Berkeley. Thesis of M. K. Go, UCRL Report No. UCRL-20483, 1971 (unpublished).

<sup>1</sup>N. Bohr, *Nature* 137, 344 (1936).

<sup>2</sup>S. N. Ghoshal, *Phys. Rev.* 80, 939 (1950).

<sup>3</sup>W. John, Jr., *Phys. Rev.* 103, 704 (1956).

<sup>4</sup>C. M. Stearns, Ph. D. thesis, Columbia University Report No. NYO-10387, 1962 (unpublished).

<sup>5</sup>S. Tanaka, M. Furukawa, S. Iwata, M. Yagi, H. Amano, and T. Mikumo, *J. Phys. Soc. Japan* 15, 2125 (1960).

<sup>6</sup>K. C. Chen and J. M. Miller, *Phys. Rev.* 134, B1269 (1964).

<sup>7</sup>C. F. Smith, Jr., Lawrence Radiation Laboratory Report No. UCRL-11862, 1965 (unpublished).

<sup>8</sup>J. M. D'Auria, M. J. Fluss, G. Herzog, L. Kowalski, J. M. Miller, and R. C. Reedy, *Phys. Rev.* 174, 1409 (1968).

<sup>9</sup>M. J. Fluss, J. M. Miller, J. M. D'Auria, N. Dudev, B. M. Foreman, Jr., L. Kowalski, and R. C. Reedy, *Phys. Rev.* 187, 1449 (1969).

<sup>10</sup>C. F. Williamson, J. P. Boujot, and J. Picard, Commissariat à l'Énergie Atomique Report No. CEA-R3042, 1966 (unpublished).

<sup>11</sup>P. G. Steward, Lawrence Radiation Laboratory Report No. UCRL-18127, 1968 (unpublished).

<sup>12</sup>J. T. Routti and S. Prussin, *Nucl. Instr. Methods* 72, 125 (1969).

<sup>13</sup>Obtained from International Atomic Energy Agency, Vienna, Austria.

<sup>14</sup>S. S. Markowitz, J. M. Miller, and G. Friedlander, *Phys. Rev.* 98, 1197 (1955).

<sup>15</sup>N. T. Porile, *Phys. Rev.* 115, 939 (1959).

<sup>16</sup>H. Hurwitz and H. A. Bethe, *Phys. Rev.* 81, 898 (1951).

<sup>17</sup>D. O. Ralieggh, Ph.D. thesis, Columbia University, 1960 (unpublished).

<sup>18</sup>For example, E. H. Auerbach, Brookhaven National Laboratory Report No. BNL-6562, 1964 (unpublished).

<sup>19</sup>J. R. Grover and R. J. Nagle, *Phys. Rev.* 134, B1269 (1964).

<sup>20</sup>T. D. Thomas, *Ann. Rev. Nucl. Sci.* 18, 343 (1968).

<sup>21</sup>D. G. Sarantites and B. D. Pate, *Nucl. Phys.* A93, 545 (1967).

<sup>22</sup>J. R. Grover, *Phys. Rev.* 127, 2142 (1962).

<sup>23</sup>D. Sperber, *Phys. Rev.* 141, 927 (1966).

<sup>24</sup>D. W. Seegmiller and K. Street, Jr., *Phys. Rev. C* 1, 695 (1970).

<sup>25</sup>J. R. Grover, *Phys. Rev.* 157, 832 (1967).

<sup>26</sup>T. Ericson and V. Strutinski, *Nucl. Phys.* 8, 284 (1958); 9, 689 (1959).

<sup>27</sup>R. Vandenbosch and J. R. Huizenga, *Phys. Rev.* 120, 1313 (1960).

<sup>28</sup>W. L. Hafner, Jr., J. R. Huizenga, and R. Vandenbosch, Argonne National Laboratory Report No. ANL-6662, 1962 (unpublished).

<sup>29</sup>T. D. Thomas, *Phys. Rev.* 116, 703 (1959).

<sup>30</sup>D. L. Hill and J. A. Wheeler, *Phys. Rev.* 89, 1102 (1953).

<sup>31</sup>J. R. Grover and J. Gilat, *Phys. Rev.* 157, 802 (1967).

<sup>32</sup>G. Friedlander, J. W. Kennedy, and J. M. Miller, *Nuclear and Radiochemistry* (Wiley, New York, 1966), 2nd ed. p. 342.

<sup>33</sup>C. C. Lu, J. R. Huizenga, C. J. Stephan, and A. J. Gorski, *Nucl. Phys.* A164, 225 (1971).

<sup>34</sup>S. M. Ferguson, H. Ejiri, and I. Halpern, *Nucl. Phys.* A188, 1 (1972).